GAZİ
JOURNAL OF ENGINEERING SCIENCES

Machinability of CoCrMo Alloy Used in Biomedical Applications: Investigation of Cutting Tool Type

Büşra Mutlu[a], Rüstem Binali[*b], Recep Demirsöz[c], Nafiz Yaşar[d]

Submitted: 10.03.2022 Revised: 05.04.2022 Accepted: 09.05.2022 doi:10.30855/gmbd.0705005

ABSTRACT

It was discovered that the machinability of CoCrMo material, which is extensively utilized in the health-care business as an implant material, may be improved through research. Three distinct cutting tools and three different cutting speeds were employed in the dry machining experiment, with three different feed rates being used in combination with three different cutting speeds (DCMT from two different firms and DCGT inserts). Cutting tools with a wide range of mechanical qualities based on hardness and toughness are available on the market today. Throughout machining, the output of a machine is defined as the average of surface roughness (Ra) and cutting temperature (T), which is estimated as the result of an experimental research conducted during the machining process. The signal-to-noise ratio (S / N) recorded during the testing was used to evaluate the results of the tests. When determining the effect of variables on Ra and T, it was determined that the Analysis of Variance (ANOVA) technique would be used. With a precision ratio of %61,4 in the analysis of variance, the feed rate was shown to be the most effective factor on Ra, while the cutting speed was found to be the most effective factor on cutting temperature (%63,9). The smallest Ra values were identified when machining at the fastest possible cutting speed and feed rate, whilst the smallest T values were obtained when machining at the slowest possible cutting speed and feed rate, respectively.

Keywords: CoCrMo, Turning, Machining, ANOVA, Regression Analysis

[a] Karabuk University,
Institute of Graduate Programs
78050 - Karabük, Türkiye
Orcid: 0000-0003-1122-7254

[b,*] Selcuk University,
Technology Faculty,
Dept. of Mechanical Engineering
42075 - Konya, Türkiye
Orcid: 0000-0003-0775-3817
e mail: rustem.binali@selcuk.edu.tr

[c] Karabuk University,
Faculty of Engineering,
Dept. of Mechanical Engineering.
78050 – Karabük, Türkiye
Orcid: 0000-0003-0674-4572

[d] Karabuk University,
Yenice Vocational High School.
78050 – Karabük, Türkiye
Orcid: 0000-0002-1427-1384

*Corresponding author:
rustem.binali@selcuk.edu.tr

Biyomedikal Uygulamalarında Kullanılan CoCrMo Alaşımının İşlenebilirliği: Kesici Takım Tipinin İncelenmesi

ÖZ

Sağlık sektöründe implant malzemesi olarak yaygın olarak kullanılan CoCrMo malzemesinin işlenebilirliğinin araştırma yoluyla geliştirilebileceği keşfedilmiştir. Üç farklı kesme hızı (iki farklı firmadan DCMT ve DCGT kesici uçlar) ile birlikte üç farklı ilerleme hızının kullanıldığı kuru işleme deneyinde üç farklı kesme takımı ve üç farklı kesme hızı kullanıldı. Bugün piyasada sertlik ve tokluğa dayalı çok çeşitli mekanik niteliklere sahip kesici takımlar mevcuttur. Talaşlı imalat boyunca, bir tezgahın çıktısı, işleme prosesi sırasında yürütülen deneysel bir araştırma sonucunda tahmin edilen yüzey pürüzlülüğü (Ra) ve kesme sıcaklığının (T) ortalaması olarak tanımlanır. Testlerin sonuçlarını değerlendirmek için test sırasında kaydedilen sinyal-gürültü oranı (S/N) kullanılmıştır. Değişkenlerin Ra ve T üzerindeki etkisi belirlenirken Varyans Analizi (ANOVA) tekniğinin kullanılacağı belirlenmiştir. Varyans analizinde %61,4 katkı oranı ile Ra üzerinde en etkili faktör ilerleme oranı gösterilirken, kesme sıcaklığı üzerinde en etkili faktör kesme hızı (%63,9) olarak bulunmuştur. En küçük Ra değerleri, mümkün olan en hızlı kesme hızı ve ilerleme hızında belirlenirken, en küçük T değerleri, mümkün olan en düşük kesme hızı ve ilerleme hızında işleme yapıldığında elde edilmiştir.

Anahtar Kelimeler: CoCrMo, Tornalama, İşleme, ANOVA, Regresyon Analizi

To cite this article: B. Mutlu, R. Binali, R. Demirsöz and N. Yaşar, "Machinability of CoCrMo Alloy Used in Biomedical Applications: Investigation of Cutting Tool Type," *Gazi Journal of Engineering Sciences,* vol. 8, no. 2, pp. 215-227, 2022. doi:10.30855/gmbd.0705005

1. Introduction

CoCrMo-based alloys used as prosthesis and implant materials are among the most important biomaterials used in medical applications [1]. Cobalt is used as an alloying element in many fields. Cobalt alloys are generally used between 650-1150 ° C. Cobalt alloys are similar in chemical structure to the stainless steel group [2]. Cobalt alloys have been used medically in dental implants obtained by the first casting method. Co-Cr consists of 65% of these alloys. Cr increases the corrosion resistance by forming protecting oxide layers on the surfaces of the alloy while Molybdenum enhances the mechanical behavior by supporting a thin structure [3,4].

CoCrMo alloys are used in the production of the hip, knee, elbow prostheses and bone plates, screws, and rods where the loading is high owing to their excellent corrosion and abrasion resistance, superior mechanical properties, and also in the production of air-jet engines, gas turbines and turbochargers, etc. due to their re-sistance to heat. By providing the surface roughness in the desired range of values, it increases the fatigue, fracture and corrosion resistance of the material as well as providing a better appearance. Today, surface roughness is one of the most significant factors in products processed by machining [5,6]. The range of surface roughness relates to the final product function where it will be used. In machining, the material structure, pro-cessing conditions and method are factors that affect the surface roughness [7–10]. Briefly, it can be described the surface roughness as fluctuations on the surface of a machined part. As the fluctuation on the surface de-creases, the surface quality of the part increases inversely [11–15]. Most of the energy required for chip removal turns into heat at the cutting edge of the cutting tool. A small portion of this heat is transferred from the cutting tool to the uncut workpiece and this process affects the surface integrity of the machined surface. Most of the heat transmitted to the workpiece remains in the chip [16] and this process causes an increase in temperature in the regions close to the cutting tool tip [12,17–19]. Some studies on the machining of CoCrMo alloys are summarized below. Bahçe et al. aimed to improve the surface integrity by using the turning and grinding of CoCrMo alloy which is a tibial component in a knee prosthesis. Comparing to the traditional turning and turning-grinding method, the surface roughness values after polishing gave similar results for the two meth-ods. They found that in the turning-grinding method, there was approximately a 64% reduction in mi-cropores/cracks and a relatively 31% reduction in microhardness [20]. Bordin et al. performed a turning pro-cess on CoCrMo alloys produced by Electron Beam Melting (EBM) method and casting method under mineral oil and water emulsion lubrication conditions using TiAlN coated tungsten carbide cutting tip. They made tool wear, surface roughness and microstructure material analysis on these alloys. They reported that CoCrMo alloy produced with EBM as a result of turning processes is more difficult to process than cast CoCrMo alloy due to its more abrasive microstructure [21]. Bruschi et al. I studied the machining properties of CoCrMo alloy (ASTM F1537). They carried out the experiments in different parameters of cutting speed and feed amounts in wet (lubricant) conditions. They investigated tool wear, surfaces integrity, microhardness and microstructure properties. According to the testing, cutting speed has no impact on the hardness of the machined surface but feed rate has an impact on tool wear and tool wear [22]. Karpuschewski et al. investigated the machinability of CoCrMo alloy during the turning process without coolant lubricant using three different ceramic cutting tools with different cutting edges. They observed that the tool life is better when the chamfer angle is small and the rake angle is large in cutting tools with two different chamfer angles and rake angle [23]. Shokrani et al. investigated tool wear and surface roughness in the machining of Co-Cr alloys in cryogenic cooling (-197 °C) environment. As a result of the experiments, it was observed that cryogenic cooling is better than Minimum Quantity Lubrication (MQL) based on the surface quality. They also observed minimum crater wear on cutting tools used in the cryogenic process [24]. Pawade et al. evaluated the cutting force components generated from the precision turning of CoCrMo alloy using different cutting parameters in different environments. They discovered that the feed force in dry machining is less than other forces, but the primary cutting force in wet machining is bigger than the other force components, according to their findings. The researchers also tested other types of cutting tools for surface integrity. They found that CBN cutting tools produced superior surface quality when compared to ceramic, carbide, and diamond cutting tools [25]. Dijmarescu et al. developed a model that demonstrates the relationship between cutting parameters (Fp, Ff and Fc) for the dry turning process of CoCrMo alloy. They emphasized that the model is acceptable since the deviation is 1.179% [26]. Karpuschewski et al. investigated the tool life, process forces and surface integrity of CoCr alloy using different cooling systems with ceramic insert. In the experiments, they performed processing experiments using dry and compressed air and three different cooling oils (kozla oil, emulsion and MQL). The minimum surface layer was formed by full jet cooled

emulsion and dry processing. In addition, they reported that low strength and low wear were caused by the MQL method [27].

When machining CoCrMo alloys under different cutting conditions, according to literature research, the surface quality and cutting forces have been taken into consideration, which is a good thing. However, in the machining of CoCrMo alloys, the cutting temperatures that have the greatest impact on tool wear have not been very noticeable. As a result, the objective of this work was to experimentally investigate the surface quality and cutting temperature of CoCrMo-based alloys that are utilized as prosthetic and implant materials.

2. Materials and Methods

2.1. Materials

The commercial CoCrMo alloy, which is widely used in knee implants and produced by casting method by Pasific medical, was used as a workpiece in turning experiments. No heat treatment has been applied to the workpiece. An original knee implant used in surgical operations was used as a workpiece material in this study as shown in Fig.1a.

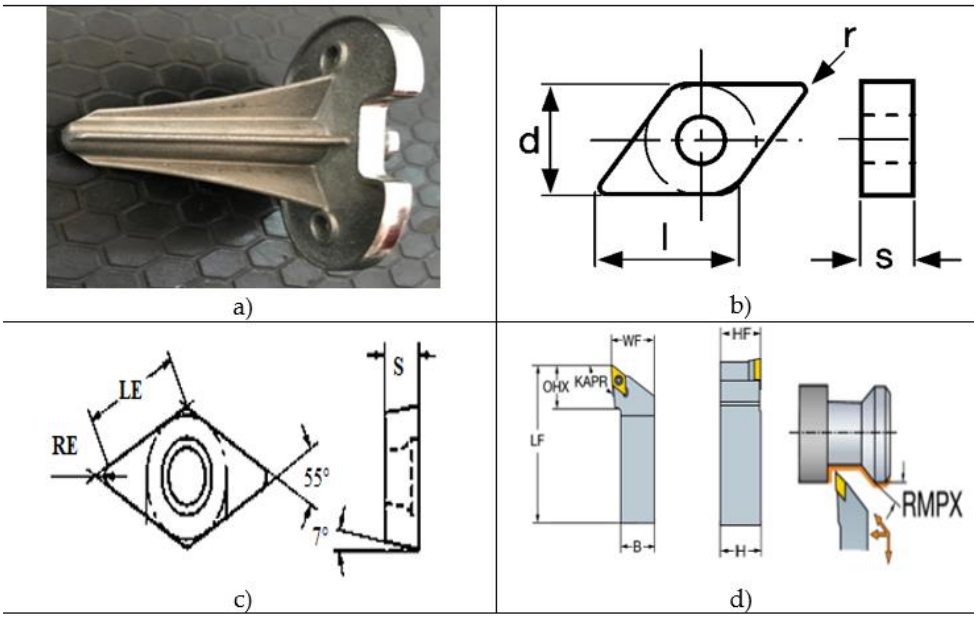

Figure 1. Test sample (Tibial component)

In the experiments, a total of three cutting tools were used: the cutting tool in DCMT form according to ISO produced by X (Fig.1b) and Y (Fig.1c) companies, and the cutting tools in DCGT (grinded tip) form belonging to Y company (Fig.1c). The cutting tools are TiAlN-based PVD coating with high-temperature hardness resistance. Also, SDJCR / L tool holder (Fig.1d) is used to connect the cutting tools to the lathe. The chemical compositions and mechanical properties of the sample are given in Table.1 During turning, temperature measurements were made with the OPTRIS PI 456 Thermal camera (OPTRIS, Berlin, Germany). In addition, Marh brand MarSurf M 300 type surface roughness measuring device was used in measuring the surface roughness.

Table 1. Chemical composition [28] and Mechanical properties [29] of CoCrMo alloy

Cr(27-30%) W(<0.2%)	**Mo(5-7%) Si(<1.0%)**	**O2(<0.1%) Ni(<0.5%)**	**Fe(<0.75%) Al(<0.1%)**	**Mg(<1.0%) Co(Balanced)**
Tensile strength (MPa)	Yield strength (MPa)	Elongation (%)	Hardness (HV)	Elastic Modulus (GPa
1263-1275	898-908	23-25	350	240-300 [3]

2.2. Tests and Measurements

Machining tests were performed on a HAAS ST-20Y CNC lathe (HAAS, Germany) with a maximum speed of 4000rpm. Therefore, suitable spindle speeds were obtained via a spindle speeder. Surface roughness

measurements as seen in Figure 2 were performed via Mahr Perthometer M300 portable measuring instrument by dividing the tibial component into 3 different regions. Roughness values were measured around the circular rings formed towards the machining center. Three measurements were taken from each of the 3 circular re-gions created to increase the stability of the measurement results and averaged. Due to the diameter difference and groove in the workpiece geometry, discontinuous turning occurs in the 1st and 2nd regions while contin-uous turning is performed in the 3rd region. Motion length (Lt) was set at 1.75 mm, and wavelength was adjusted at 0.8 mm in the Marsurf M300 measuring instrument for surface roughness measurements It was determined by averaging variances in roughness profile on machined surfaces according to the ISO 4287 standard. The measurement of surface roughness was performed on the machined surface by three repetitions and then taken the average of these repetitions. The experimental setup where turning tests are carried out is shown in Figure 3.

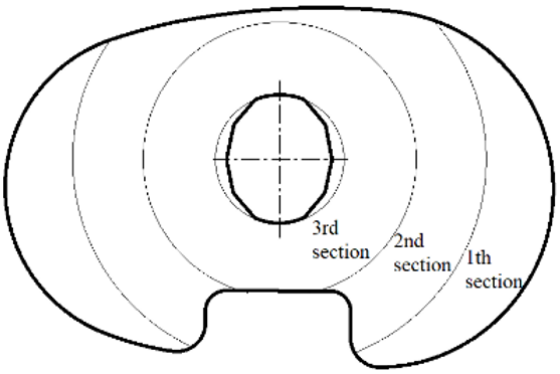

Figure 2. Surface roughness measurement

During turning, the temperature at the tool-workpiece zone was constantly measured using an OPTRIS PI 450 infrared (IR) thermal camera. The IR camera can measure temperatures up to 900 ° C, it has a 7.5-13 µm spec-tral range, 40mK thermal sensitivity and 382x288 pixel resolution.

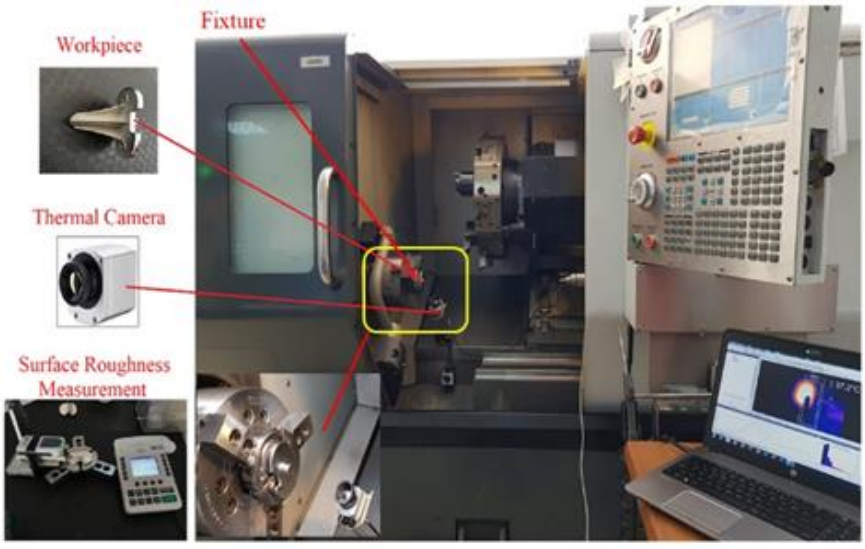

Figure 3. Experimental setup and schematic diagram

2.3. Design of Experiments

Taguchi optimization is a method based on testing many factors with the least factor with orthogonal arrays defined in the experimental design created. Orthogonal arrays are determined in two or three stages according to the nature of the problem. Taguchi L27 full factorial array was used in this study. S/N ratio is determined differently to determine the best value in experiment design. In the study, the smaller-better ratio was preferred among the S/N ratios. The equation of the chosen ratio is given below, and in the equation, Y represents the quality variable. The cutting parameters and their levels

are given in Table 2. The full Taguchi L27 array is given in Table 3.

The smaller-The better

$$S/N\ ratio \quad = \quad -10 * log(\Sigma(1/Y2)/n) \tag{1}$$

Table 2. Parameters and levels for experimental turning

Symbols	Factors	Level 1	Level 2	Level 3
T	Cutting Tool	DCMT (X Companies)	DCMT (Y Companies)	DCGT (Y Companies)
V	Cutting speed (m/min)	40	60	80
f	Feed rate (mm/rev)	0.05	0.075	0.1
a	Deep of cut (mm)	0.1	0.1	0.1

Table 3. Taguchi L27 array

Exp. No	Code	Cutting Tool	Code	Cutting Speed (m/min)	Code	Feed Rate (mm/rev)
1	T1	X Comp.	V1	40	f1	0.05
2	T1	X Comp.	V1	40	f2	0.075
3	T1	X Comp.	V1	40	f3	0.10
4	T1	X Comp.	V2	60	f1	0.05
5	T1	X Comp.	V2	60	f2	0.075
6	T1	X Comp.	V2	60	f3	0.10
7	T1	X Comp.	V3	80	f1	0.05
8	T1	X Comp.	V3	80	f2	0.075
9	T1	X Comp.	V3	80	f3	0.10
10	T2	Y Comp.	V1	40	f1	0.05
11	T2	Y Comp.	V1	40	f2	0.075
12	T2	Y Comp.	V1	40	f3	0.10
13	T2	Y Comp.	V2	60	f1	0.05
14	T2	Y Comp.	V2	60	f2	0.075
15	T2	Y Comp.	V2	60	f3	0.10
16	T2	Y Comp.	V3	80	f1	0.05
17	T2	Y Comp.	V3	80	f2	0.075
18	T2	Y Comp.	V3	80	f3	0.10
19	T3	Y Comp.	V1	40	f1	0.05
20	T3	Y Comp.	V1	40	f2	0.075
21	T3	Y Comp.	V1	40	f3	0.10
22	T3	Y Comp.	V2	60	f1	0.05
23	T3	Y Comp.	V2	60	f2	0.075
24	T3	Y Comp.	V2	60	f3	0.10
25	T3	Y Comp.	V3	80	f1	0.05
26	T3	Y Comp.	V3	80	f2	0.075
27	T3	Y Comp.	V3	80	f3	0.10

3. Results and Discussion

3.1. Analysis of S/N ratios

Ra is shown as one of the most critical parameters as machinability output in machining operations [31,32]. In addition, the temperature that occurs in the cutting region during machining is another considerable parameter affecting surface quality and the tool performance [33,34]. For this reason, optimizing the surface roughness and temperature generated during the machining process is very important for machinability efficiency. Turning performance tests were completed based on Taguchi's L27 full factorial design using cutting tool, cutting speed and feed rate control factors. Table 4 gives the Ra and T outputs obtained as a result of the experiments and the S / N ratios obtained from the analysis result. The smallest-best approximation was used to obtain S / N ratios by using Equation 1. Consequently, the average surface roughness (Ra) value was obtained as 0.680 µm and the average S / N ratio as 3.68 dB. For the cutting temperature, the average temperature (T) value was 199 °C and the

average S / N ratio was -45.88 dB.

Table 4. Experiment results (Ra and T) and S / N ratios

Exp. No	Cutting Tool	Cutting Speed (m/min)	Feed Rate (mm/rev)	Surface Roughness Ra (µm)	Surface Ropughness S/N	Average Temperature (°C)	Temperature S/N (dB)
1	T1	V1	f1	0.597	4.480513	152	-43.6369
2	T1	V1	f2	0.792	2.025496	168	-44.5062
3	T1	V1	f3	1.131	-1.06925	180	-45.1055
4	T1	V2	f1	0.494	6.125461	175	-44.8608
5	T1	V2	f2	0.718	2.877511	191	-45.6207
6	T1	V2	f3	0.904	0.876631	202	-46.107
7	T1	V3	f1	0.455	6.839772	218	-46.7691
8	T1	V3	f2	0.599	4.451464	235	-47.4214
9	T1	V3	f3	0.774	2.225181	251	-47.9935
10	T2	V1	f1	0.612	4.264972	160	-44.0824
11	T2	V1	f2	0.773	2.23641	191	-45.6207
12	T2	V1	f3	1.168	-1.34886	198	-45.9333
13	T2	V2	f1	0.518	5.713405	203	-46.1499
14	T2	V2	f2	0.755	2.441061	225	-47.0437
15	T2	V2	f3	0.948	0.463833	234	-47.3843
16	T2	V3	f1	0.486	6.267275	235	-47.4214
17	T2	V3	f2	0.615	4.222498	249	-47.924
18	T2	V3	f3	0.793	2.014536	265	-48.4649
19	T3	V1	f1	0.513	5.797653	138	-42.7976
20	T3	V1	f2	0.601	4.422511	149	-43.4637
21	T3	V1	f3	0.929	0.639686	160	-44.0824
22	T3	V2	f1	0.453	6.878036	157	-43.918
23	T3	V2	f2	0.537	5.400514	201	-46.0639
24	T3	V2	f3	0.684	3.298878	213	-46.5676
25	T3	V3	f1	0.408	7.786797	196	-45.8451
26	T3	V3	f2	0.511	5.831582	214	-46.6083
27	T3	V3	f3	0.607	4.336226	236	-47.4582

The S/N analysis table created with the Taguchi method is given in Table 5. According to the S / N response table, the best level was found according to the smallest S / N ratio within each control factor's levels. Accordingly, the control factors and levels for the lowest Ra (surface roughness) value were determined as T3V3f1 and for T (temperature), T3V1f1.

Table 5. S/N responses for surface roughness Ra and cutting temperature T

	Surface roughness (Ra)			Cutting temperature (T)		
Levels	**T**	**V**	**f**	**T**	**V**	**f**
1	0,7182	0,7907	**0,5040**	196,9	**166,2**	**181,6**
2	0,7409	0,6679	0,6557	217,8	200,1	202,6
3	**0,5826**	**0,5831**	0,8820	**184,9**	233,2	215,4
Delta	0,1583	0,2076	0,3780	32,9	67,0	33,9
The order of importance	3	2	1	3	1	2

*Data shown in bold are optimum conditions.

S/N ratios for Ra and T are given in Figures 4a and 4b, respectively. The levels with the smallest S/N ratios are seen in the graphs as the optimum level. Considering the smallest S/N ratios, the optimum Ra value is achieved with the DCGT (T3) tool at V3 and f1. Considering the smallest S/N ratio, it is seen that the DCGT (T3) tool, V1 and f1 are the ideal values for the T value. The graphic trends also give an idea about the effect levels of the factors. The most important factors are the feed rate and the cutting speed for the Ra and T, respectively based on Fig. 4a and 4b.

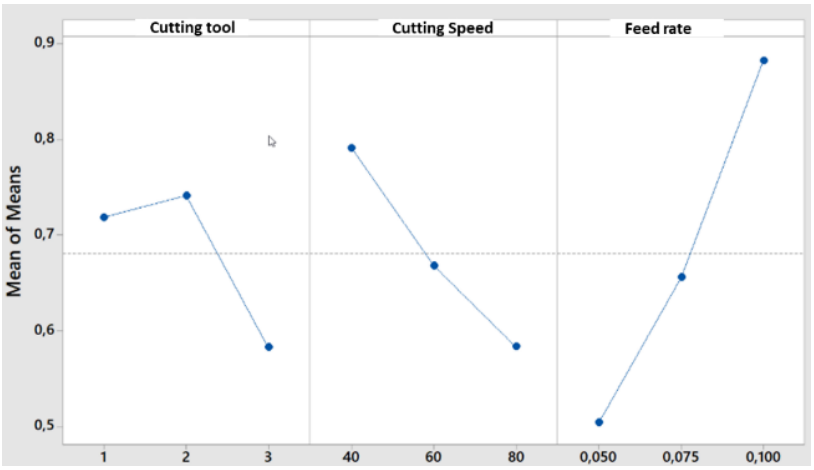

(a)

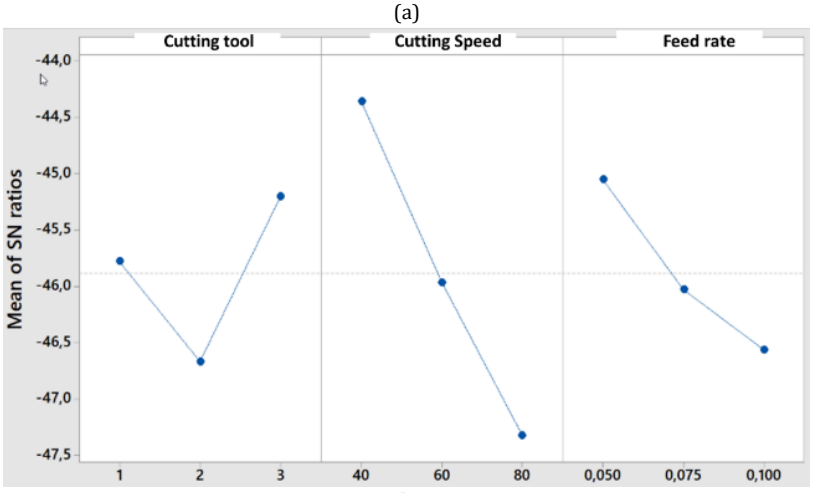

(b)

Figure 4. Main effect plots of S / N ratios for (a) Surface roughness Ra, (b) Temperature T

3.2. Analysis of Variance (ANOVA)

The influence of cutting parameters on Ra and T was determined using an ANOVA with a 95 percent confidence interval. Using the chart's contribution rates, you can see how much of an impact the control factor has on output. Analysis findings for the Ra and T variances may be seen in Table 6.

Table 6. ANOVA analysis results for Ra and T

Factor	Degree of Freedom (DF)		Sum-of-Squares (SS)		Mean-Square (MS)		F ratio		P value		Percentage Contribution Ratio (PCR%)	
	Ra	T	Ra	T	Ra	T	Ra	T	Ra	T	Ra	T
T	2	2	0.13197	6.3373	0.065983	3.1686	178.80	50.21	0.000	0.000	12.44	15.8
V	2	2	0.19602	25.6209	0.098011	12.8104	265.59	202.97	0.000	0.000	18.47	63.9
f	2	2	0.65134	6.7545	0.325670	3.3772	882.51	53.51	0.000	0.000	61.4	16.84
T * V	4	4	0.00418	0.5545	0.001045	0.1386	2.83	2.20	0.098	0.160	0.39	1.38
T * f	4	4	0.02153	0.1521	0.005383	0.0380	14.59	0.60	0.001	0.672	2.02	0.37
V * f	4	4	0.05281	0.1656	0.013203	0.0414	35.78	0.66	0.000	0.639	4.97	0.41
Error	8	8	0.00295	0.5049	0.000369	0.0631	-	-	-	-	0.27	1.25
Total	26	26	1.06080	40.0897	-	-	-	-	-	-	%100	%100
R2				Ra						T		
				99.72						98.74		

Considering the data in Table 6, it has been determined that the most efficient factor for Ra is the f (feed rate) with 61.4% PCR. The most effective factors in the second and third place are the V (cutting speed) and the T (cutting tool) with 18.42% and 12.44% PCR, respectively. According to Table 6, the most influential factor on the cutting temperature with 63.9% PCR is the V (cutting speed), followed by the f (feed rate) and the T (cutting tool) with 16.84% and 15.8% PCR, respectively.

3.3. Evaluation of Ra

In the performance experiments, the influence of the parameters (cutting speed and feed rate) on Ra for each tool is given in the graphics in Figure 5. If Figure 5a is examined for the T1 cutting tool, it is seen that it gives the best Ra value (0.455 µm) at V3 and f1. The highest value in terms of Ra was found as 1.131 µm at V3 and f2. When the Ra graphs for the tools are evaluated, the Ra value decreases inversely by increasing cutting speed. Better surface quality is obtained with the increasing cutting speed in machining as known. The reason for this can be explained by the decrease in friction due to the decrease in the tool chip interface by the increasing cutting speed and the increasing temperature decreases the materials strength [35,36]. In addition, when the graphs were examined, it is obvious that the Ra value increased with the increasing feed rate. During the machining process, the feed rate directly affects the cross-section of the chip that the cutting tool removes per unit time. With the increasing feed rate, the chip cross-section area increases and the slip plane in the first deformation zone increase with the increasing chip cross-section, more force is required for the cutting process and the cutting process becomes more difficult [37].

In the literature, the Ra value increases with the increasing feed rate [22,38-40]. This situation confirms that the most effective factor obtained in the variance analysis is the feed rate with 61.4% PCR. When Figure 5b is examined for T2 cutting tool, it is seen that there is no significant difference in terms of Ra values with T1 cutting tool with the same form. The lowest Ra value is 0.486 µm at V3 and f1. The highest Ra value is 1.168µm at V1 and f2.

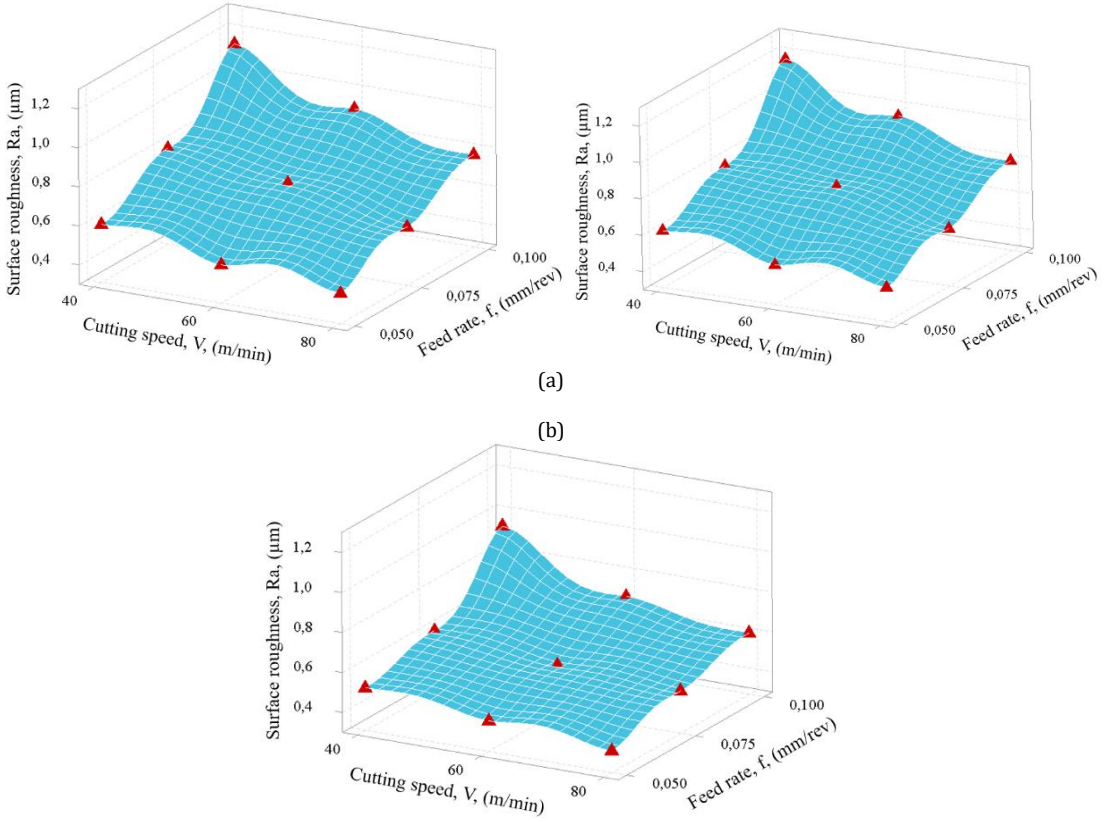

Figure 5. Surface roughness variation for (a) T1 (b) T2 (c) T3 cutting tools ((a) T1 (b) T2 (c) T3)

It is known that the area between the cutting tool/workpiece surface decreases with the increase of the rake angle in machining, so the friction is less and the cutting process is easier [41,42], Since the T3 cutting tool with a grinded tip is larger than the other T1 and T2 cutting tools used, better surface

qualities have been obtained. This statement is frequently encountered in studies in the literature [42,43]. When Figure 5c is examined for the T3 cutting tool, the best surface roughness value is 0.408 µm at V3 and f1. The highest Ra value was obtained as 0.929µm at V1 and f2. From Figure 7.5, the most effective parameter in the T3 cutting tool is the feed rate. Figure 5 confirms that according to the S/N table, the best result for the surface roughness value will be obtained with the T3 cutting tool. Consequently, the better Ra values will be acquired by using the tip ground cutting tools.

3.4. Evaluation of Temperature

In the machining process, the temperature caused by friction between the surface and the tool reduces the machining quality by penetrating (sticking) to the surface more than necessary if the temperature is higher than desired [43]. This situation makes the cutting temperature one of the very important parameters for a required cutting process. The effect of cutting parameters on T for each tool in performance experiments is given in the graphics in Figure 6. When Figure 6a is examined for the T1 cutting tool, the lowest cutting temperature is obtained as 152 ° C at V1 and f2. While chip removal is taking place, the cutting tool and workpiece's contact area grows. In other words, as the area of contact between the cutting tool and the workpiece grows, so does the cutting temperature. Figure 6a demonstrates that cutting speed does not cause a significant rise in temperature. However, with the increase in the feed, the cutting temperature increased proportionally. This situation confirms that based on the ANOVA results, the parameter that has the highest effect on the cutting temperature is the cutting speed with 63.9% PCR. When Figure 6b and 6c are examined, it is seen that this situation is valid for T2 and T3 tools. Moreover, the lowest temperature value is 160 °C and 138 °C, respectively, at V1 and f2, while the highest temperature value is obtained as 265 °C and 236 °C, at V3 and f2. When Figure 6c is examined for the T3 tools, it is seen that the temperature increase is less than the other two sets of the tools. This situation is thought to be caused by the T3 cutting tool tip being ground. It is known in the literature that the increase in the rake angle and decrease in the effective surface between the tool and workpiece generates less friction and heat during the process [42]. Accordingly, the rake angle of the insert with grinded T3 is larger than the other tools, resulting in less cutting temperature during machining.

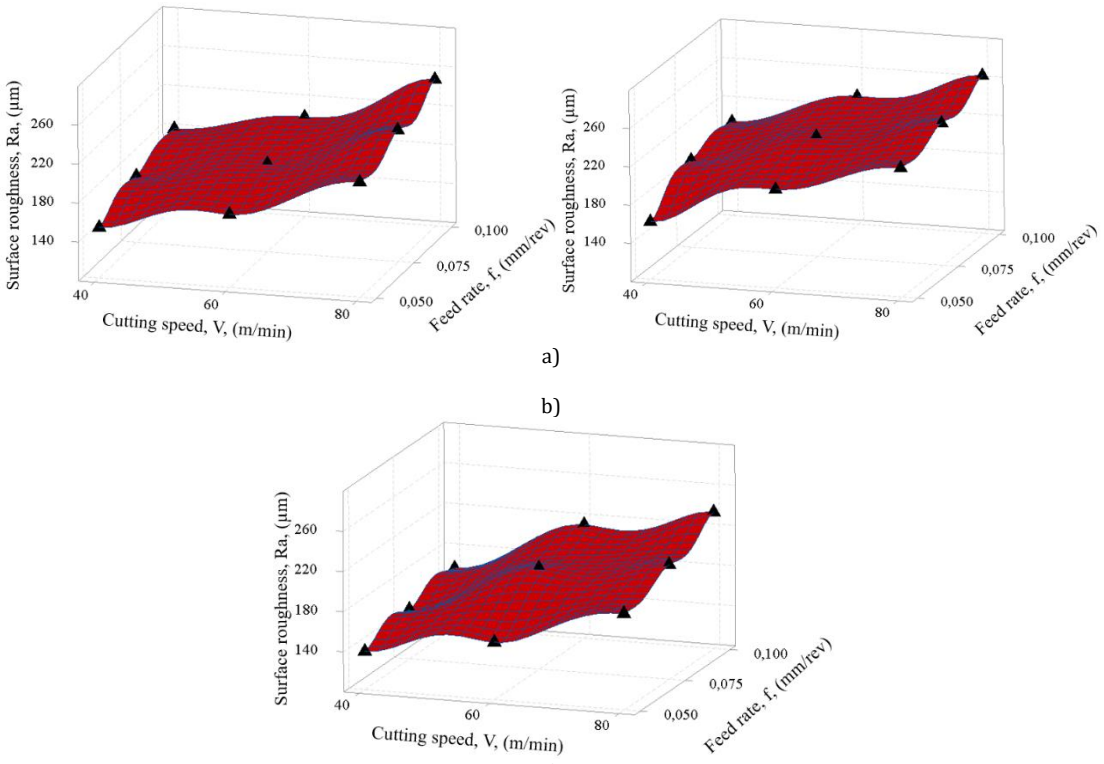

Figure 6. Cutting temperature variation for (a) T1 (b) T2 (c) T3 cutting tools ((a) T1 (b) T2 (c) T3)

3.5. Tool Performance

Figure 7 depicts the relationship between the amount of wear on the cutting tool side surface area and

the amount of surface roughness that occurs during the turning of the same material with varied mechanical qualities while using different cutting tools with varying mechanical properties. It was discovered that the lowest possible surface roughness was attained during the turning of the sample with the T3 cutting tool that possessed the maximum toughness, while the least amount of tool wear was seen in parallel. The opposite was true while creating the maximum roughness value during turning with T1 and T2 cutting tools of lesser toughness. As a result, greater tool wear occurred during turning. Surface roughness and tool wear are reduced in this scenario while turning the same material, since the toughness of the cutting tool improves with increasing toughness of the material [44].

At the tool-chip interface, as a result of the forces acting during the cutting process, the heat has been generated along the contact area due to friction, causing tool wear. It is necessary to know the maximum temperature and temperature distribution that are decisive in tool wear [45,46]. It is so important to accurately measure and determine the heat and temperature distribution at the tool-chip interface for estimating the tool wear. Since the depth of cut is so small in this study and results in higher cutting temperature at the slip zone and the tool-chip interface [47], it is so important to measure the temperature distribution formed here in a way that reflects the tool wear. By this context, the temperature caused by the friction between the cutting tool and the workpiece in the chip removal process played a major role in tool wear, depending on the material properties of the workpiece and the cutting tool [48]. Generally, factors such as increasing cutting speed, feed rate and also are known to increase the cutting temperature and cause tool wear [49,50]. With the help of Figure 6 and Figure 7b, the higher tool wear occurs with T2 tool causing the highest cutting temperature in machining of CoCrMo alloy.

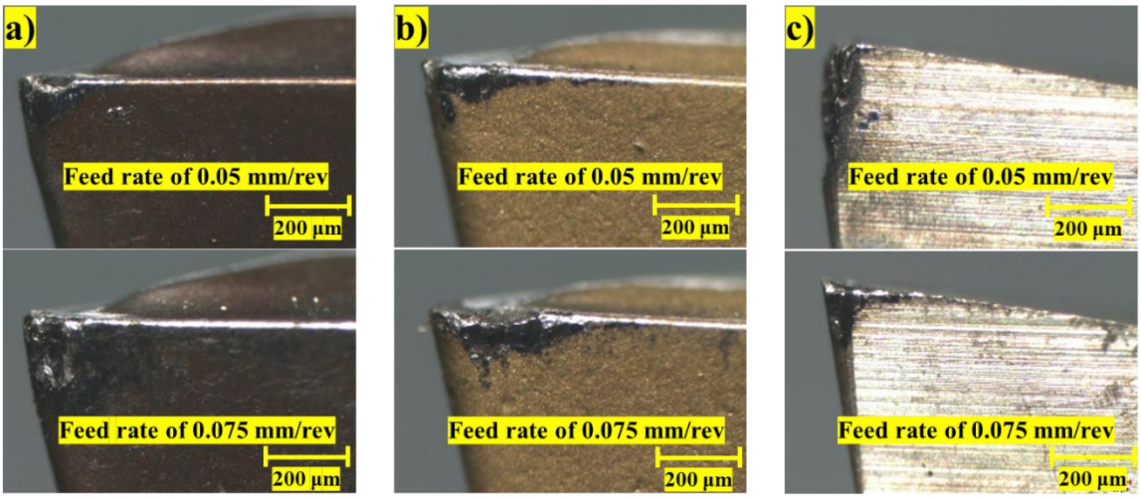

Figure 7. Tool wear images of different cutting tools in the cutting speed of 40 m/min, a) T1, b) T2, c) T3

4. Conclusion

For the machining of CoCrMo implant material (biomaterial), Taguchi L27 was used to explore the impact of the machining parameters on the Ra and the T (cutting tool, cutting speed, and feed rate). The experiments' outcomes are summarized in the following paragraphs.

There are statistically optimal Ra values at V3 and f1 for cutting tools of DCMT (X companies), DCMT (Y companies) and DCGT (Y companies), respectively, based on the statistical study. It is found that the maximum surface roughness values for each tool factors are at V1 and f2 for V1 and f2. Temperatures of 152, 160, and 138 ºC are the best values for each DCMT (X companes), DCMT (Y companies), and the DCGT (Y comepanies) tool, respectively at V1 and f2. With DCMT (X companies), DCMT (Y companies), and DCGT (Y companies) cutting tools, V3 and f2 show the maximum cutting temperatures of 251, 265, and 236 °C. S/N ratios were utilized to determine the ideal Ra and T values. The statistical analysis determined that the best Ra value could be obtained at V3 and f1 using the DCGT (Y companies) cutting tool. At V1 and f1, the DCGT (Y companies) cutting tool produced the best T values.

According to the ANOVA results, the feed rate on the Ra has a PCR efficiency of %61.4. Furthermore, the T's cutting speed has the highest PCR at %63.9.

Cutting speed increased the surface roughness and the cutting temperature, according to the results. A little rise in cutting temperature has been seen when feed rate is increased. This raises surface roughness correspondingly.

Cutting tools with tip ground (DCGT (Y companies)) tips were found to provide the greatest results on Ra and T. It can be used to improve the quality of the surface.

Acknowledgment

This research was funded by Karabük University, grant number KBÜBAP-18-YL-189.

Conflict of Interest Statement

The authors declare that there is no conflict of interest.

References

[1] E. Şap and H. Çelik, "Investigation of Effects of Ti and Mn Addition on Microstructure and Mechanical Properties of Cobalt Based Alloys," *Electronic Journal of Machine Technologies*, vol. 9, no. 3, pp. 25–33, 2012.

[2] E. Şap, "Investigation of effects of some metals on cobalt-based alloys," Fırat University Graduate School of Natural and Applied Sciences, 2010.

[3] I. Milošev, *Biomedical Applications: CoCrMo Alloy for Biomedical Applications,* Ed. Boston, MA: Springer US, 2012.

[4] E. Bahce, M. S. Güler, E. Emir, and C. Özel, "CoCrMo Tibial Komponentin Karbür Takı m ile İşlenmesinde Yüzey Özelliklerinin Araştırılması," *Ordu University Journal of Science and Technology*, vol. 8, no. 1, pp. 16–30, 2018.

[5] H. Gökçe, İ. Çiftçi, H. Demir, "Cutting parameter optimization in shoulder milling of commercially pure molybdenum," *Journal of the Brazilian Society of Mechanical Sciences and Engineering*, pp. 40–360, 2018. doi:10.1007/s40430-018-1280-8

[6] M. E. Korkmaz and M. Günay, "Experimental and Statistical Analysis on Machinability of Nimonic80A Superalloy with PVD Coated Carbide," *Sigma Journal of Engineering and Natural Sciences*, vol. 36, no. 4, pp. 1141–1152, 2018.

[7] A. T. Abbas, D. Y. Pimenov, I. N. Erdakov, M. A. Taha, M. S. Soliman, and M. M. El Rayes, "ANN surface roughness optimization of AZ61 magnesium alloy finish turning: Minimum machining times at prime machining costs," *Materials*, vol. 11, no. 5, 2018. doi:10.3390/ma11050808

[8] A. T. Abbas, D. Y. Pimenov, I. N. Erdakov, M. A. Taha, M. M. El Rayes, and M. S. Soliman, "Artificial intelligence monitoring of hardening methods and cutting conditions and their effects on surface roughness, performance, and finish turning costs of solid-state recycled aluminum alloy 6061 chips," *Metals,* vol. 8, no. 6, 2018, doi:10.3390/met8060394

[9] M. S. Alajmi and A. M. Almeshal, "Modeling of Cutting Force in the Turning of AISI 4340 Using Gaussian Process Regression Algorithm," *Applied Sciences*, vol. 11, no. 9. 2021. doi:10.3390/app11094055

[10] M. Kuntoğlu, A. Aslan, D. Y. Pimenov, K. Giasin, T. Mikolajczyk, and S. Sharma, "Modeling of Cutting Parameters and Tool Geometry for Multi-Criteria Optimization of Surface Roughness and Vibration via Response Surface Methodology in Turning of AISI 5140 Steel," *Materials*, vol. 13, no. 19. 2020. doi:10.3390/ma13194242

[11] M. K. Gupta, M. Mia, G. R. Singh, D. Y. Pimenov, M. Sarikaya, and V. S. Sharma, "Hybrid cooling-lubrication strategies to improve surface topography and tool wear in sustainable turning of Al 7075-T6 alloy," *International Journal of Advanced Manufacturing Technology,* vol. 101, no. 1–4, pp. 55–69, 2019. doi:10.1007/s00170-018-2870-4

[12] M. Mia and N. R. Dhar, "Optimization of surface roughness and cutting temperature in high-pressure coolant-assisted hard turning using Taguchi method," *The International Journal of Advanced Manufacturing Technology*, pp. 739–753, 2017. doi:10.1007/s00170-016-8810-2

[13] G. Manimaran, S. Anwar, M. A. Rahman, M. E. Korkmaz, M. K. Gupta, A. Alfaify, and M. Mia, "Investigation of surface modification and tool wear on milling Nimonic 80A under hybrid lubrication," *Tribology International*, vol. 155, p. 106762, 2021. doi:10.1016/j.triboint.2020.106762

[14] M. Günay, M. E. Korkmaz, and N. Yaşar, "Performance analysis of coated carbide tool in turning of Nimonic 80A superalloy under different cutting environments," *Journal of Manufacturing Processes,* vol. 56, pp. 678–687, 2020. doi:10.1016/j.jmapro.2020.05.031

[15] M. A. Erden, N. Yaşar, M. E. Korkmaz, B. Ayvacı, K. Nimel Sworna Ross, and M. Mia, "Investigation of microstructure,

mechanical and machinability properties of Mo-added steel produced by powder metallurgy method," *The International Journal of Advanced Manufacturing Technology*, 2021, doi:10.1007/s00170-021-07052-z

[16] M. E. Korkmaz and Nafiz Yaşar, "FEM modelling of turning of AA6061-T6: Investigation of chip morphology, chip thickness and shear angle," *Journal of Production Systems and Manufacturing Science*, vol. 2, no. 1, pp. 50–58, 2021.

[17] M. Mia and N. R. Dhar, "Response surface and neural network based predictive models of cutting temperature in hard turning," *Journal of Advanced Research*, vol. 7, no. 6, pp. 1035–1044, 2016. doi:10.1016/j.jare.2016.05.004

[18] M. Mia and N. R. Dhar, "Effects of duplex jets high-pressure coolant on machining temperature and machinability of Ti-6Al-4V superalloy," *Journal of Materials Processing Technology*, vol. 252, pp. 688–696, 2018. doi:10.1016/j.jmatprotec.2017.10.040

[19] M. E. Korkmaz and M. Günay, "Finite Element Modelling of Cutting Forces and Power Consumption in Turning of AISI 420 Martensitic Stainless Steel," *Arabian Journal for Science and Engineering,* vol. 43, no. 9, pp. 4863–4870, 2018, doi:10.1007/s13369-018-3204-4

[20] E. Bahçe, M. S. Güler, and E. Emir, "Investigation of surface quality of CoCrMo alloy used in the tibial component of the knee prosthesis according to the methods of turning and turning-grinding," *Materials Science*, vol. 26, no. 1, pp. 41–48, 2020, doi:10.5755/j01.ms.26.1.21729

[21] A. Bordin, A. Ghiotti, S. Bruschi, L. Facchini, and F. Bucciotti, "Machinability Characteristics of Wrought and EBM CoCrMo Alloys," *Procedia CIRP*, vol. 14, pp. 89–94, 2014. doi: https:10.1016/j.procir.2014.03.082

[22] S. Bruschi, A. Ghiotti, and A. Bordin, "Effect of the process parameters on the machinability characteristics of a CoCrMo Alloy," *Key Engineering Materials*, vol. 554–557, pp. 1976–1983, 2013. doi:10.4028/www.scientific.net/KEM.554-557.1976

[23] B. Karpuschewski and J. Döring, "Influence of the Tool Geometry on the Machining of Cobalt Chromium Femoral Heads," *Procedia CIRP*, vol. 49, pp. 67–71, 2016. doi:10.1016/j.procir.2015.07.034

[24] A. Shokrani, V. Dhokia, and S. T. Newman, "Cryogenic High-Speed Machining of Cobalt Chromium Alloy," *Procedia CIRP*, vol. 46, pp. 404–407, 2016. doi:10.1016/j.procir.2016.04.045

[25] K. Jagtap and R. Pawade, "A Comparative Analysis of Cutting Forces in Precision Turning of Co-Cr-Mo Bio-implant Alloy in Dry and Wet Machining Environments," *Advances in Intelligent Systems Research,* vol. 137, pp. 234–241, 2017. doi:10.2991/iccasp-16.2017.38

[26] M. R. Dijmarescu, T. D. Popovici, I. C. Tarba, M. C. Dijmarescu, and C. F. Bisu, "An experimental study on cutting forces when machining a CoCrMo alloy," *IOP Conference Series: Materials Science and Engineering*, vol. 400, no. 2, 2018. doi:10.1088/1757-899X/400/2/022019

[27] B. Karpuschewski, H. J. Pieper, and J. Döring, "Impact of the cooling system on the cutting of medical cobalt chromium with ceramic cutting inserts," *Production Engineering*, vol. 8, no. 5, pp. 613–618, 2014. doi:10.1007/s11740-014-0559-6

[28] G. Matula, A. Szatkowska, K. Matus, B. Tomiczek, and M. Pawlyta, "Structure and Properties of Co-Cr-Mo Alloy Manufactured by Powder Injection Molding Method," *Materials*, vol. 14, no. 8. 2021. doi: 10.3390/ma14082010

[29] Y. Okazaki, A. Ishino, and S. Higuchi, "Chemical, Physical, and Mechanical Properties and Microstructures of Laser-Sintered Co–25Cr–5Mo–5W (SP2) and W–Free Co–28Cr–6Mo Alloys for Dental Applications," *Materials*, vol. 12, no. 24. 2019. doi:10.3390/ma12244039

[30] H. R. Kim, S. H. Jang, Y. K. Kim, J. S. Son, B. K. Min, K. H. Kim, and T. Y. Kwon, "Microstructures and Mechanical Properties of Co-Cr Dental Alloys Fabricated by Three CAD/CAM-Based Processing Techniques," *Materials*, vol. 9, no. 7. 2016. doi:10.3390/ma9070596

[31] M. Özdemir, "Analysis of the Effect Rates of Cutting Parameters on Surface Roughness using Surface Response Method," *Gazi University Science Journal: PART: C Design and Technology*, vol. 7, no. 3, pp. 639–648, 2019. doi:10.29109/gujsc.595722

[32] K. Leksycki, E. Feldshtein, G. M. Królczyk, and S. Legutko, "On the Chip Shaping and Surface Topography When Finish Cutting 17-4 PH Precipitation-Hardening Stainless Steel under Near-Dry Cutting Conditions," *Materials,* vol. 13, no. 9. 2020. doi:10.3390/ma13092188

[33] O. Çakır, M. Kıyak, and E. Altan, "Comparison of gases applications to wet and dry cuttings in turning," *Journal of Materials Processing Technology*, vol. 153–154, pp. 35–41, 2004. doi:10.1016/j.jmatprotec.2004.04.190

[34] Y. Yamane, N. Narutaki, and K. Hayashi, "Suppression of tool wear by using an inert gas in face milling," *Journal of Materials Processing Technology*, vol. 62, no. 4, pp. 380–383, 1996. doi:10.1016/S0924-0136(96)02439-9

[35] P. Fallböhmer, C. A. Rodríguez, T. Özel, and T. Altan, "High-speed machining of cast iron and alloy steels for die and mold manufacturing," *Journal of Materials Processing Technology*, vol. 98, no. 1, pp. 104–115, 2000. doi:10.1016/S0924-0136(99)00311-8

[36] B. Özlü, M. Akgün, and H. Demir, "AA6061 Alaşımının tornalanmasında kesme parametrelerinin yüzey pürüzlülüğü üzerine etkisinin analizi ve optimizasyonu," *Gazi Mühendislik Bilimleri Dergisi*, vol.5, no. 2, pp. 151-158, 2019. doi:10.30855/gmbd.2019.02.04

[37] A. Takmaz, "Optimization By The Taguchi Method Of Effect On The Surface Roughness Of Cryogenic Treatment Applied To Cutting Tools," *Düzce University*, 2018.

[38] A. Bordin, S. Bruschi, and A. Ghiotti, "The Effect of Cutting Speed and Feed Rate on the Surface Integrity in Dry Turning of CoCrMo Alloy," *Procedia CIRP*, vol. 13, pp. 219–224, 2014. doi:10.1016/j.procir.2014.04.038

[39] M. R. Dijmarescu, M. C. Dijmarescu, I. Voiculescu, T. D. Popovici, and I. C. Tarba, "Study on the influence of cutting parameters on surface quality when machining a CoCrMo alloy," *IOP Conference Series: Materials Science and Engineering*, vol. 400, no. 2, 2018. doi:10.1088/1757-899X/400/2/022020

[40] R. Çakıroğlu, and G. Uzun, "Yüksek ilerleme ile frezeleme işlemi esnasında oluşan kesme kuvvetinin ve iş parçası yüzey pürüzlülüğünün yapay sinir ağları ile modellenmesi," *Gazi Mühendislik Bilimleri Dergisi*, vol. 7, no. 1, pp. 58-66, 2021, doi:10.30855/gmbd.2021.01.07

[41] M. Günay, İ. Korkut, E. Aslan, and U. Şeker, "Experimental investigation of the effect of cutting tool rake angle on main cutting force," *Journal of Materials Processing Technology*, vol. 166, no. 1, pp. 44–49, 2005, doi:10.1016/J.JMATPROTEC.2004.07.092

[42] M. Sekmen, M. Günay, and U. Şeker, "Effect on Formations of Built-up Edge and Built-up Layer, Surface Roughness of Cutting Speed and Rake Angle in the Machining of Aluminum Alloys," *Journal of Polytechnic*, vol. 18, no. 3, pp. 141–148, 2015.

[43] N. A. Abukhshim, P. T. Mativenga, and M. A. Sheikh, "Heat generation and temperature prediction in metal cutting: A review and implications for high speed machining," *International Journal of Machine Tools and Manufacture*, vol. 46, no. 7, pp. 782–800, 2006, doi:10.1016/j.ijmachtools.2005.07.024

[44] I. Campos, M. Farah, N. López, G. Bermúdez, G. Rodríguez, and C. VillaVelázquez, "Evaluation of the tool life and fracture toughness of cutting tools boronized by the paste boriding process," *Applied Surface Science*, vol. 254, no. 10, pp. 2967–2974, 2008. doi:10.1016/j.apsusc.2007.10.038

[45] M. S. I. Chowdhury, B. Bose, S. Rawal, G. S. Fox-Rabinovich, and S. C. Veldhuis, "Investigation of the Wear Behavior of PVD Coated Carbide Tools during Ti6Al4V Machining with Intensive Built Up Edge Formation," *Coatings,* vol. 11, no. 3. 2021. doi:10.3390/coatings11030266

[46] M. Yavuz, H. Gökçe, and U. Şeker, "Matkap geometrisinin takım aşınması ve talaş oluşumu üzerine etkisinin araştırılması," *Gazi Mühendislik Bilimleri Dergisi*, vol. 3, no. 1, 2017.

[47] S. Sulaiman, A. Roshan, and S. Borazjani, "Effect of cutting parameters on cutting temperature of TiAL6V4 alloy," *Applied Mechanics and Materials*, vol. 392, pp. 68–72, 2013, doi:10.4028/www.scientific.net/AMM.392.68

[48] J. Yuan, J. M. Boyd, D. Covelli, T. Arif, G. S. Fox-Rabinovich, and S. C. Veldhuis, "Influence of Workpiece Material on Tool Wear Performance and Tribofilm Formation in Machining Hardened Steel," *Lubricants*, vol. 4, no. 2. 2016. doi:10.3390/lubricants4020010

[49] E. Şap, Ü. A. Usca, M. K. Gupta, M. Kuntoğlu, M. Sarıkaya, D. Y. Pimenov, and M. Mia, "Parametric Optimization for Improving the Machining Process of Cu/Mo-SiCP Composites Produced by Powder Metallurgy," *Materials*, vol. 14, no. 8. 2021. doi:10.3390/ma14081921

[50] M. F. Ghazali, M. M. A. B. Abdullah, S. Z. Abd Rahim, J. Gondro, P. Pietrusiewicz, S. Garus, T. Stachowiak, A. Victor Sandu, M. Faheem Mohd Tahir, M. E. Korkmaz and M. S. Osman, "Tool Wear and Surface Evaluation in Drilling Fly Ash Geopolymer Using HSS, HSS-Co, and HSS-TiN Cutting Tools," *Materials,* vol. 14, no. 7, p. 1628, 2021, doi:10.3390/ma14071628